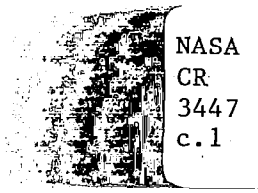

NASA Contractor Report 3447

Turbulent Flow in a Square-to-Round Transition

A. M. K. P. Taylor, J. H. Whitelaw,
and M. Yianneskis

CONTRACT NASW-3258
JULY 1981

NASA

NASA Contractor Report 3447

Turbulent Flow in a Square-to-Round Transition

A. M. K. P. Taylor, J. H. Whitelaw,
and M. Yianneskis
Imperial College of Science and Technology
London, England

Prepared for
Lewis Research Center
under Contract NASW-3258

National Aeronautics
and Space Administration

Scientific and Technical
Information Branch

1981

TABLE OF CONTENTS

SUMMARY

Turbulent flow in a duct in which the cross-section undergoes a transition from square to round has been measured at a Reynolds number of 35 350. The hydraulic diameter, 40 mm, was the same in the square inlet and round exit sections, resulting in a cross-sectional area reduction of 21.5%. The transition takes place over two hydraulic diameters. Laser Doppler velocimetry was used to measure the streamwise and secondary mean velocity components and the associated turbulence levels and cross-correlations in stations upstream of, in, and downstream of the transition. The results provide an understanding of the flow and assist the evaluation of numerical techniques.

The boundary layers at inlet and exit of the transition were approximately 13% and 20% respectively of the hydraulic diameter. Thickening of the boundary layers at the duct corners is associated with the secondary flow away from the corner fillets and along the duct walls, towards the duct midplanes. Cross-stream velocities of up to 7% of the bulk velocity were measured; the secondary flow is produced by the longitudinal curvature of the wall and the related pressure gradients.

1. INTRODUCTION

Flows in ducts which change cross-sectional area and shape are used in a wide range of engineering configurations and this report is concerned with the flow in a transition from a square to a circular cross-section with a decrease in area of 21.5% over two hydraulic diameters. The lateral convergence of the flow is accompanied by the generation of cross-stream velocities, or secondary motions, which result from the pressure field.

In long ducts of square section, secondary flows of the "second kind" arise and are driven by gradients of Reynolds-stresses with a magnitude of less than 1.5% of the bulk flow velocity: see, for example, reference 1. In the present flow the turbulent boundary layers at the inlet to the transition piece are thin and it can be expected that any secondary flows of the second kind will be much less than, say, 1% of the bulk flow velocity. Any larger cross-stream velocity within the transition piece stems from the change in cross-sectional shape and the related cross-stream pressure gradients.

The measurements of reference 3 provide some information of the flow in a transition from a rectangular to a circular section (and vice versa) with no change in cross-sectional area. The data includes contours of streamwise isotachs and the streamwise pressure variation. Two configurations were investigated in which the transition occurred over 0.69 and 2.76 hydraulic diameters and it is evident that the length of the transition is influential on the flow development. For example, cross-stream velocities presented for the round-to-rectangular transitions reached maxima of about 0.18 and 0.09 of the maximum streamwise velocity for the short and long transition ducts respectively. For the rectangular entry sections, the flows were fully developed at the inlet to the transition ducts and thus stress-driven secondary flows were also present.

The flow investigated in this report is relevant to the case of aircraft intake ducts. The measurements are intended to quantify the mean and fluctuating components of the streamwise and cross-stream velocities of the flow and so provide better understanding and a basis for the testing of design methods. In common with the previous investigations of references 1 and 2, laser Doppler velocimetry was used to measure the velocity components.

The following section describes the experimental procedure and section 3 presents the measurements. Concluding remarks are provided in section 4.

2. FLOW CONFIGURATION AND INSTRUMENTATION

The transition from a 40 mm square cross-section to a 40 mm diameter circular cross-section took place in a duct length of 80 mm. The duct is

depicted in figure 1 together with the coordinate system adopted in the report. Each cross-section in the transition is formed by the intersection of a square and a circle, which resembles, to within 1.5% of the radius a super ellipse with a shape factor of unity. The radius of the circle decreases linearly along the transition from 28.28 mm to 20.00 mm. The transition piece was installed in the water tunnel previously used in reference 2. The bulk velocity through the square section was 0.885 m/s which corresponds to a Reynolds number of 35 350, based on the hydraulic diameter. The temperature of the water was maintained at 20 $\pm$ 2° C for all the experiments. Measurements of velocity were restricted by limits of optical access, caused by refraction at curved surfaces within the transition piece and in the downstream pipe.

The optical arrangement of the laser Doppler velocimeter was identical to that of reference 2. Doppler signals were processed by a frequency-tracking demodulator (Cambridge Consultants CC01). A careful appraisal of the measurement errors has already been made in reference 2, where the precision (random error) of the mean and fluctuating components of velocity was assessed as $\pm$ 1½% and from $\pm$ 1½% to $\pm$ 5% respectively. In interpreting the results of the next section, it is important to note that the accuracy (systematic error) of the secondary velocity components is limited by the alignment of the velocimeter to the duct (see reference 1). The resulting systematic error is not more than 0.008 V_c.

3. RESULTS AND DISCUSSION

Symmetry tests on the streamwise flow in the duct upstream of the transition piece were carried out, with the result that measurements at equivalent locations on either side of the symmetry plane of the duct agreed within the precision of the measurement.

Figure 1 shows the development of the streamwise velocity on the centreline of the duct. The velocity increases from 1.12 V_c upstream of the transition to 1.43 downstream, as a consequence of the decrease in cross-section. Figures 2a-2e show profiles of the streamwise mean velocity, U, and the corresponding root mean square velocity, $\tilde{u}$, at a number of stations upstream, within and downstream of the transition piece. The boundary layer thickness on the symmetry plane, defined at 95% of the maximum velocity, is about 13% of the hydraulic diameter at the inlet to the transition piece (figure 2a), but rises to about 20% at the exit (figure 2d). The change in the profiles is comparatively small, as would be expected from the centreline change in figure 1. Careful examination of the profiles near the sidewalls shows that the fluid near the planes x_2/D and x_3/D = 0 accelerates relative to that near to the fillets which form the transition, and that the boundary layers are thinner away from the fillets. The profiles of $\tilde{u}$ (and $\tilde{v}$, figure 2f) are those expected for a turbulent wall boundary layer.

Figure 3 presents profiles of the cross-stream velocity for three stations within the transition piece. The measurements quantify the symmetry about planes at 45^{o} to the x_2 or x_3 planes, which is within the limits of the systematic error discussed in section 2, as are the magnitudes of the cross-stream velocities on the symmetry planes (x_2/D or $x_3/D=0$). The measurements show that large values of the cross-stream velocity are found close to the walls and to the fillets which form the transition from the square to the circular cross-section. The largest values shown are of the order of 0.07 V_c, although the shape of the profile suggests that the maximum lies closer to the wall than $x_3/D\simeq0.9$. The magnitude and direction of these velocities indicates that their source is pressure-gradient - rather than Reynolds stress-gradient. The direction of the cross-stream velocities is always away from the channel diagonal (line A-A' on figure 4) and thus cannot satisfy continuity in the cross-stream plane. This implies an acceleration of the streamwise velocity component near the symmetry planes (lines B-B' on figure 4) which is indeed observed, particularly in figure 2(c).

The origin of the lateral pressure-gradient, which drives the cross-stream flow, is due to the increase in pressure near the fillet relative to that in the region of the symmetry planes. This increase is brought about by the streamline curvature occurring in planes containing the channel diagonal and the duct centre-line upon entry to the transition piece, as shown in fig. 4 (a). In contrast, no such curvature occurs with streamlines contained in planes such as that depicted in Fig. 4 (b). It is noted that this mechanism should be reversed on exit from the transition piece and can be expected to cause the rapid decay of the cross-stream components.

These lateral pressure variations were also observed by Mayer (3); the qualitative changes in pressure and the related secondary flow directions are in accordance with the above discussion. However the simultaneous occurrence of longitudinal convergence on one wall and divergence on the other wall of the transition duct results in cross-stream flows not directly comparable to those presented in this report.

An order-of-magnitude estimation of the affect of curvature, given in Appendix 2, suggests secondary flow velocities not more than 0.16 of the bulk velocity. This is, considering the crude nature of the analysis, in good agreement with experiment.

Measurements of the $\overline{uw}$ and $\overline{uv}$ cross correlations were also obtained. As expected they were very low ($< 0.2 \times 10^{-3} V_c^2$) over the central region of the flow, rising to about $0.5 \times 10^{-3} V_c^2$ near the sidewalls. These values are close to the limits of accuracy of the velocimeter and are thus not presented.

The results from which the figures have been plotted are tabulated in Appendix 1.

4. CONCLUDING REMARKS

1. The experiments have quantified the streamwise and cross-stream velocities in a square to circular transition piece with thin inlet boundary layers.

2. The streamwise boundary layers assume smaller thicknesses away from the fillets which form the transition piece. The cross-stream velocity profiles are consistent with this observation; magnitudes of $\simeq 0.07$ of the bulk velocity have been measured.

3. The secondary velocities are driven by cross-stream pressure gradients induced by the longitudinal curvature of the streamlines on passing through the transition piece.

4. Because of the importance of wall curvature, its accurate representation is crucial to the calculation of the flow.

APPENDIX 1 - TABULATED DATA

TABLE I - SQUARE-TO-ROUND TRANSITION MEAN VELOCITY, TURBULENCE LEVEL MEASUREMENTS

REYNOLDS NUMBER 35,350

(All quantities normalised by the bulk velocity, V_c = 0.885 m/s)

D_H	$\frac{x_2}{D}$	$\frac{x_3}{D}$	$\bar{U}/V_c$	$\tilde{u}/V_c$ x10^2	D_H	$\bar{U}/V_c$	$\tilde{u}/V_c$	D_H	$\bar{U}/V_c$	$\tilde{u}/V_c$ x10^2
-2.0	0.0	0.0	1.118	0.721	-1.0	1.136	0.721	0.0	1.145	0.722
		0.1	1.118	0.721		1.136	0.721		1.145	0.768
		0.2	1.118	0.721		1.136	0.721		1.145	0.811
		0.3	1.118	0.721		1.136	0.721		1.145	0.839
		0.4	1.118	0.721		1.136	0.811		1.145	0.901
		0.5	1.118	0.946		1.133	1.117		1.138	1.533
		0.6	1.107	2.389		1.116	2.636		1.109	3.426
		0.7	1.050	4.704		1.068	5.273		1.025	5.409
		0.8	0.964	6.200		0.964	6.698		0.960	6.220
		0.9	0.865	7.341		0.879	7.910		0.865	7.697
3.0	0.0	0.0	1.421	0.914	4.0	1.430	0.959			
		0.1	1.421	0.914		1.430	0.959			
		0.2	1.421	0.959		1.432	1.005			
		0.3	1.421	1.074		1.435	1.188			
		0.4	1.414	1.736		1.427	1.873			
		0.5	1.391	3.290		1.400	3.610			
		0.6	1.343	4.769		1.352	4.769			
		0.7	1.288	5.636		1.297	5.636			
		0.8	1.220	6.214		1.220	6.503			
		0.9	1.119	7.949		1.087	9.683			

D_H	$x_{2/D}$	$x_{3/D}$	$\bar{u}/v_c$	$\tilde{u}/v_c$ x10^2	$\bar{v}/v_c$ x10^2	$\tilde{v}/v_c$ x10^2	$\bar{w}/v_c$ x10^2	$\tilde{w}/v_c$ x10^2
1.0	0.0	0.0	1.199	0.766	-0.646	0.572	-0.637	0.867
		-0.1	1.199	0.811	-0.646	0.682	-0.637	0.867
		-0.2	1.199	0.766	-0.646	0.706	-0.637	0.867
		-0.3	1.197	0.856	-0.807	0.725	-0.637	0.867
		-0.4	1.194	0.991	-0.646	0.862	-0.797	1.068
		-0.5	1.190	1.690	-0.646	1.646	-0.797	2.134
		-0.6	1.158	3.516	-0.807	2.433	-0.637	3.584
		-0.7	1.098	5.341	-0.646	4.327	-0.797	4.886
		-0.8	1.003	6.693	-0.807	5.327	-0.637	5.288
		-0.9	0.901	6.761	-0.807	-	-0.637	5.685
1.0	0.25	0.0	1.194	0.901	-0.646	0.745	-0.637	0.819
		-0.1	1.194	0.901	-0.606	0.719	-0.637	0.819
		-0.2	1.194	0.946	-0.646	0.765	-0.637	0.959
		-0.3	1.194	1.127	-0.646	0.778	-0.637	0.959
		-0.4	1.193	1.149	-0.646	1.098	-0.637	1.066
		-0.5	1.183	2.118	-0.646	1.698	-0.637	1.753
		-0.6	1.158	3.516	-1.055	3.568	0.000	3.231
		-0.7	1.091	5.612	-0.969	4.301	0.000	5.048
		-0.8	1.010	6.761	-2.642	5.409	1.530	5.171
		-0.9	0.885	7.843	-3.232	5.557	3.188	5.546
1.0	0.50	0.0	1.172	1.680	-0.646	2.042	-0.159	2.050
		-0.1	1.172	1.805	-0.646	1.805	-0.159	2.203
		-0.2	1.174	2.251	-0.646	1.953	0.000	2.209
		-0.3	1.179	2.299	-0.646	2.150	-0.159	2.475
		-0.4	1.172	2.411	-0.969	1.850	-0.159	2.147
		-0.5	1.167	3.074	-1.131	2.444	0.556	2.721
		-0.6	1.127	4.395	-1.707	3.280	0.797	3.186
		-0.7	1.055	5.950	-2.262	4.316	2.231	4.472
		-0.8	0.960	7.234	-3.706	5.334	3.188	5.613
		-0.9	0.842	7.978	-5.171	5.601	5.206	6.168
1.50	0.0	0.0	1.255	0.811	-0.323	0.626	-0.318	0.819
		-0.1	1.260	0.811	-0.646	0.626	-0.318	1.005
		-0.2	1.260	0.811	-0.646	0.626	-0.318	0.968
		-0.3	1.255	0.901	-0.323	0.609	-0.318	1.096
		-0.4	1.249	1.262	-0.646	0.691	-0.318	1.230
		-0.5	1.246	1.848	-0.646	2.307	-0.318	2.303
		-0.6	1.217	3.651	-0.484	3.700	-0.797	3.778
		-0.7	1.145	5.544	-0.807	4.533	-0.797	5.026
		-0.8	1.066	6.558	-0.807	5.648	-0.797	5.719
		-0.9	0.964	7.572	-0.807	6.154	-0.797	2.689
		-0.95	0.824	11.630	-0.807	5.475	-0.797	

*For the $\bar{w}$ and $\tilde{w}$ measurements the absolute values of the coordinate $x_{2/D}$ correspond to $-x_{3/D}$ and of the coordinate $x_{3/D}$ to $x_{2/D}$.

D_H	$x_{2/D}$	$x_{3/D}$	$\overline{U}/V$	$\tilde{u}/V_c$ x10^2	$\overline{V}/V_c$ x10^2	$\tilde{v}/V_c$ x10^2	$\overline{W}/V_c$ x10^2	$\tilde{w}/V_c$ x10^2
1.50	0.25	0.0	1.258	0.856	-0.646	0.672	-0.318	1.051
		-0.1	1.258	0.856	-0.646	0.699	-0.318	1.051
		-0.2	1.258	0.901	-0.646	0.719	-0.159	1.033
		-0.3	1.258	0.946	-0.517	0.765	-0.159	1.051
		-0.4	1.258	1.217	-0.646	1.142	-0.159	1.678
		-0.5	1.246	2.254	-0.807	2.145	-0.159	2.369
		-0.6	1.201	4.327	-0.969	2.943	-0.159	3.698
		-0.7	1.140	5.612	-1.454	4.834	0.478	5.175
		-0.8	1.055	6.693	-2.544	5.373	1.594	5.367
		-0.9	0.947	7.532	-4.124	5.982	3.188	5.803
1.50	0.325	0.0	1.274	1.059	-0.646	1.054	-0.318	1.051
		-0.1	1.274	1.037	-0.646	1.147	-0.318	1.051
		-0.2	1.271	1.082	-0.646	1.122	-0.318	1.051
		-0.3	1.274	1.172	-0.807	1.119	-0.159	1.149
		-0.4	1.269	1.442	-0.969	1.443	0.398	1.548
		-0.5	1.254	2.817	-1.311	2,561	0.669	2.337
		-0.6	1.195	5.000	-2.101	3.583	1.147	3.515
		-0.7	1.123	6.355	-3.236	5.067	2.550	4.903
		-0.8	1.029	7.201	-4.871	5.783	4.622	5.717
		-0.9	0.926	7.883	-7.195	6.048	6.694	6.244
1.75	0.0	0.0	1.316	0.901				
		-0.1	1.316	0.901				
		-0.2	1.316	0.946				
		-0.3	1.316	0.991				
		-0.4	1.311	1.442				
		-0.5	1.293	3.110				
		-0.6	1.253	4.703				
		-0.7	1.189	5.986				
		-0.8	1.113	6.699				
		-0.9	1.036	7.269				
1.75	0.125	0.0	1.307	0.856	-0.646	0.719	-0.478	0.872
		-0.1	1.307	0.901	-0.646	0.745	-0.478	0.961
		-0.2	1.307	0.901	-0.646	0.773	-0.318	0.959
		-0.3	1.307	0.991	-0.646	0.786	-0.318	1.005
		-0.4	1.307	1.127	-0.646	1.210	-0.159	1.883
		-0.5	1.298	2.402	-0.807	1.743	0.000	2.248
		-0.6	1.256	4.192	-1.417	3.542	0.318	4.235
		-0.7	1.197	5.544	-2.101	4.955	1.274	5.482
		-0.8	1.121	7.572	-3.210	5.487	2.039	5.589
		-0.9	1.030	8.056	-3.393	5.784	3.505	6.139

D_H	$x_{2/D}$	$x_{3/D}$	$\overline{U}/V_c$	$\tilde{u}/V_c$ x10^2	$\overline{V}/V_c$ x10^2	$\tilde{v}/V_c$ x10^2	$\overline{W}/V_c$ x10^2	$\tilde{w}/V_c$ x10^2
1.75	0.25	0.0	1.307	0.946	-0.646	-	0.015	-
		-0.1	1.307	0.946	-0.646	-	0.015	-
		-0.2	1.307	1.014	-0.646	-	0.015	
		-0.3	1.307	1.104	-0.807	-	0.337	
		-0.4	1.302	1.532	-0.807	-	0.467	
		-0.5	1.284	3.178	-1.660	-	1.146	
		-0.6	1.239	4.847	-2.224	-	1.377	
		-0.7	1.181	6.130	-3.334	-	2.422	
		-0.8	1.086	7.271	-5.171	-	4.302	
		-0.9	0.987	7.984	-7.093	-	6.697	

APPENDIX 2

Estimation of the cross-stream pressure variation

Referring to figure 5, consider the centripetal force balance due to the streamline curvature for the fluid particle shown :

$$\delta m \frac{V^2}{R} = \delta p \ (\delta x \cdot \delta y) \qquad (1)$$

{where · $\delta m = \rho(\delta x \cdot \delta y \cdot \delta r)$ is the mass of the fluid particle,
· δp is the difference in pressure across the particle in the r direction
· R is the radius of curvature of the streamline}

Hence

$$\rho \frac{V^2}{R} = \frac{\delta p}{\delta r} \qquad (2)$$

Using the following approximations

$$V \simeq U_B$$

$$\frac{\delta p}{\delta r} \simeq \frac{p_2 - p_1}{D/2}$$

{where · U_B is a representative streamwise velocity,
· D is the hydraulic diameter of the duct
· p_2 and p_1 are defined in figure 5}

$$p_2 - p_1 \simeq \rho \frac{U_B^2}{R} \frac{D}{2} \qquad (3)$$

Considering motion in the cross-stream plane (refer to figure 4 (c)) and applying Bernoulli's equation between points near the fillet and points near $x_2 = x_3 \simeq D$

$$\Delta U \simeq \left(\frac{p_2 - p_1}{\frac{1}{2}\rho} \right)^{\frac{1}{2}} \qquad (4)$$

{where ΔU is the induced cross-stream velocity}

Eliminating the term for $(p_2 - p_1)$ in (4) using (3) there results

$$\Delta U \simeq \left(\frac{U_B^2 D}{R} \right)^{\frac{1}{2}}$$

$$\frac{\Delta U}{U_B} \simeq 0.2 \left(\frac{1}{R} \right)^{\frac{1}{2}}, \text{ for } D = 0.04 \text{ m.} \qquad (5)$$

An estimate for R, derived in figure 5, is R > 1·5 m. and hence $\frac{\Delta U}{U_B} < 0.16$: Viscous forces will act so as to lessen the magnitude further still.

APPENDIX 3 - NOMENCLATURE

D	defined as $D_H/2$
D_H	hydraulic diameter (40mm)
U	mean component along X_1 co-ordinate direction
$\tilde{u}$	r.m.s. component along X_1 co-ordinate direction
$\overline{uv}$	cross correlation of fluctuation in $X_1 \sim X_2$ plane
$\overline{uw}$	cross correlation of fluctuation in $X_1 \sim X_3$ plane
V	mean component along X_2 co-ordinate direction
V_c	bulk mean velocity defined in square section
$\tilde{v}$	r.m.s. component along X_2 co-ordinate direction
W	mean component along X_3 co-ordinate direction
$\tilde{w}$	r.m.s. component along X_3 co-ordinate direction
X_1, X_2, X_3	defined in figure 1

REFERENCES

1. Melling, A., and Whitelaw, J.H., (1976), "Turbulent Flow in a Rectangular Duct", J. Fluid Mech., 78, 289.

2. Taylor, A.M.K.P., Whitelaw, J.H., and Yianneskis, M., (1980), "Measurements of Laminar and Turbulent Flow in a Curved Duct with Thin Inlet Boundary Layers", report submitted as NASA Contractor Report.

3. Mayer, E., (1938), "Einfluss der Querschnittsverformung auf die Entwicklung der Geschwindigkeits- und Druckverteilung bei turbulenten Strömungen in Rohren", VDI-Forschungsheft 389.

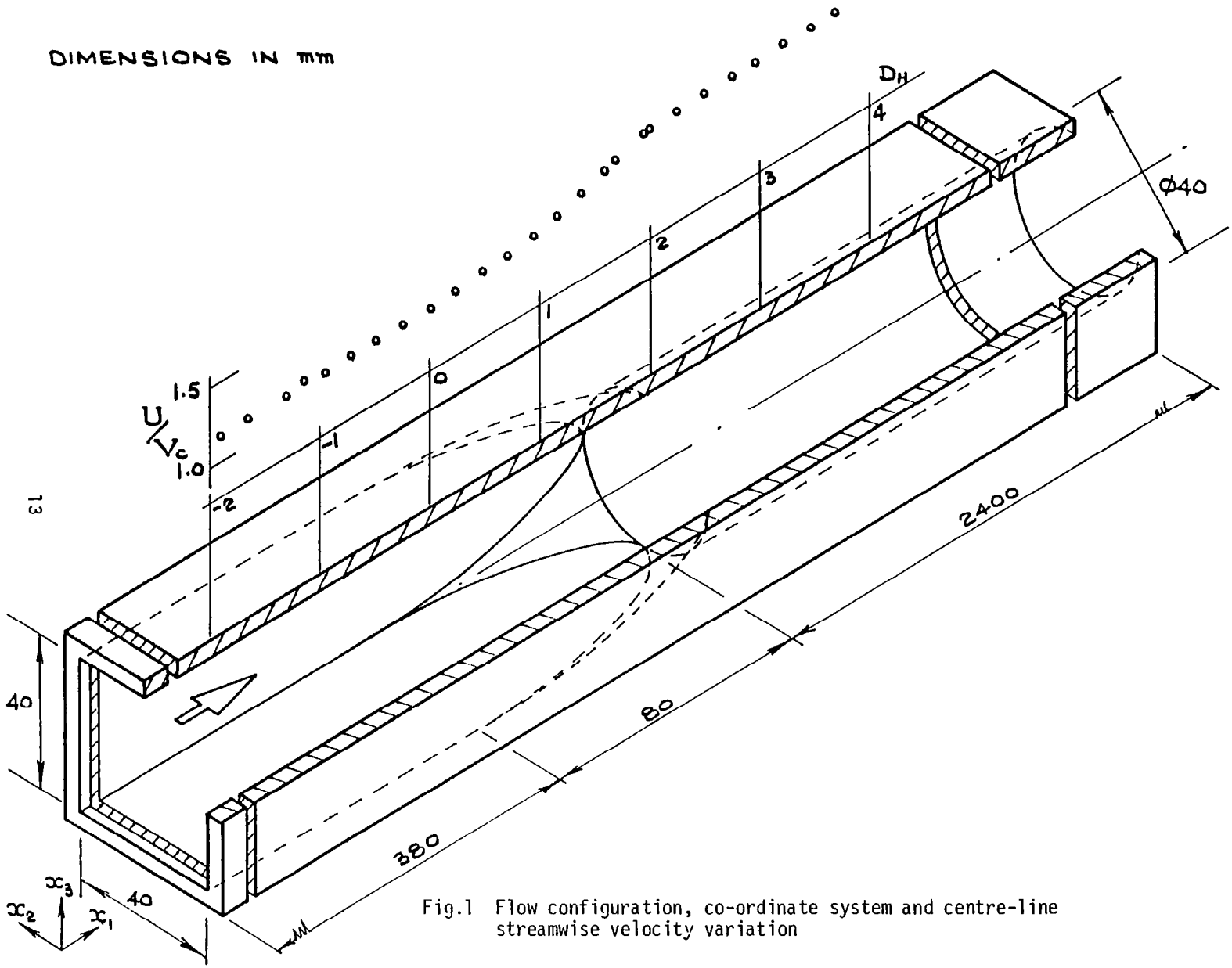

Fig.1 Flow configuration, co-ordinate system and centre-line streamwise velocity variation

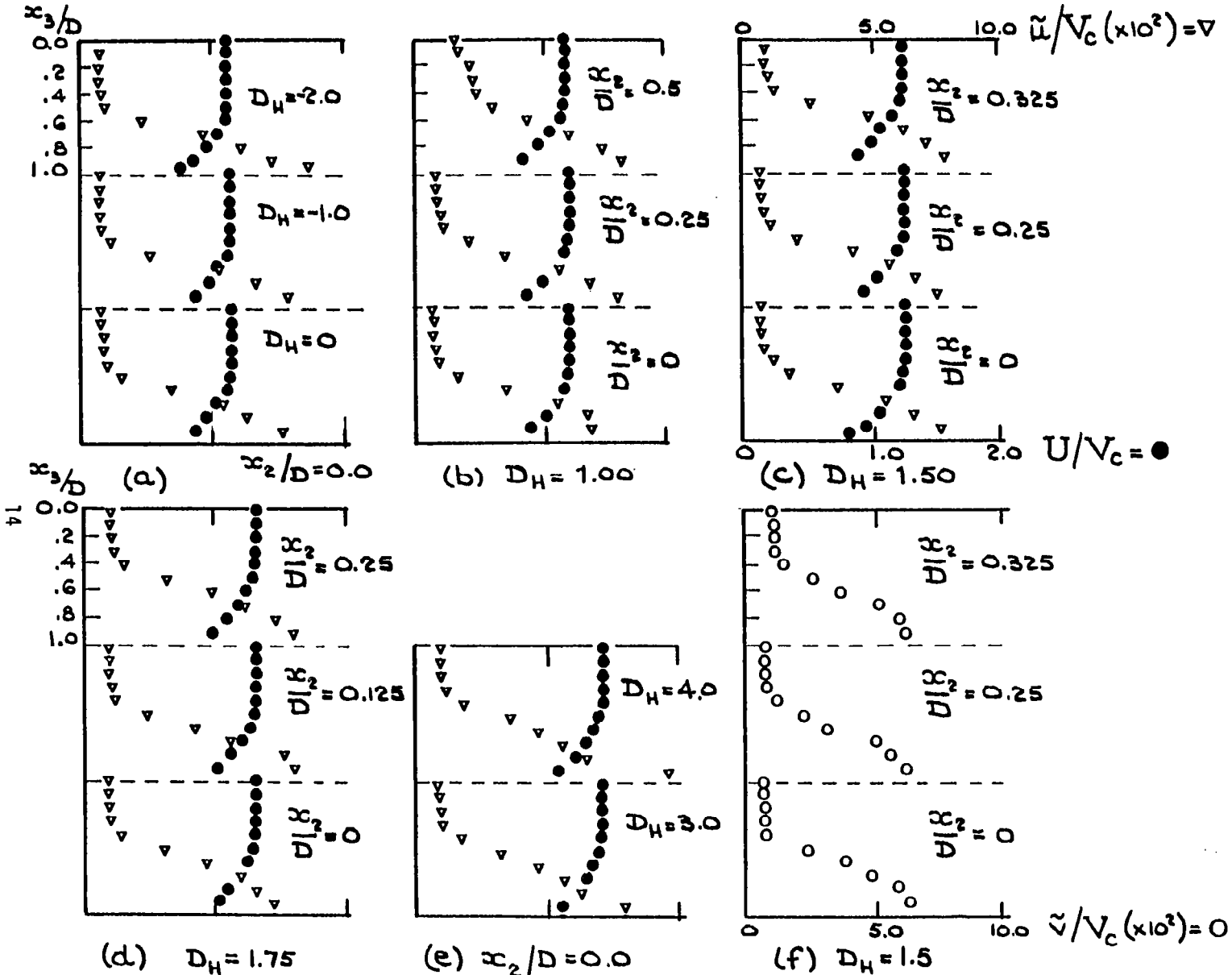

Fig.2 (a)-(e) : Streamwise velocity profiles and turbulence levels;
(f) : Cross-stream turbulence levels

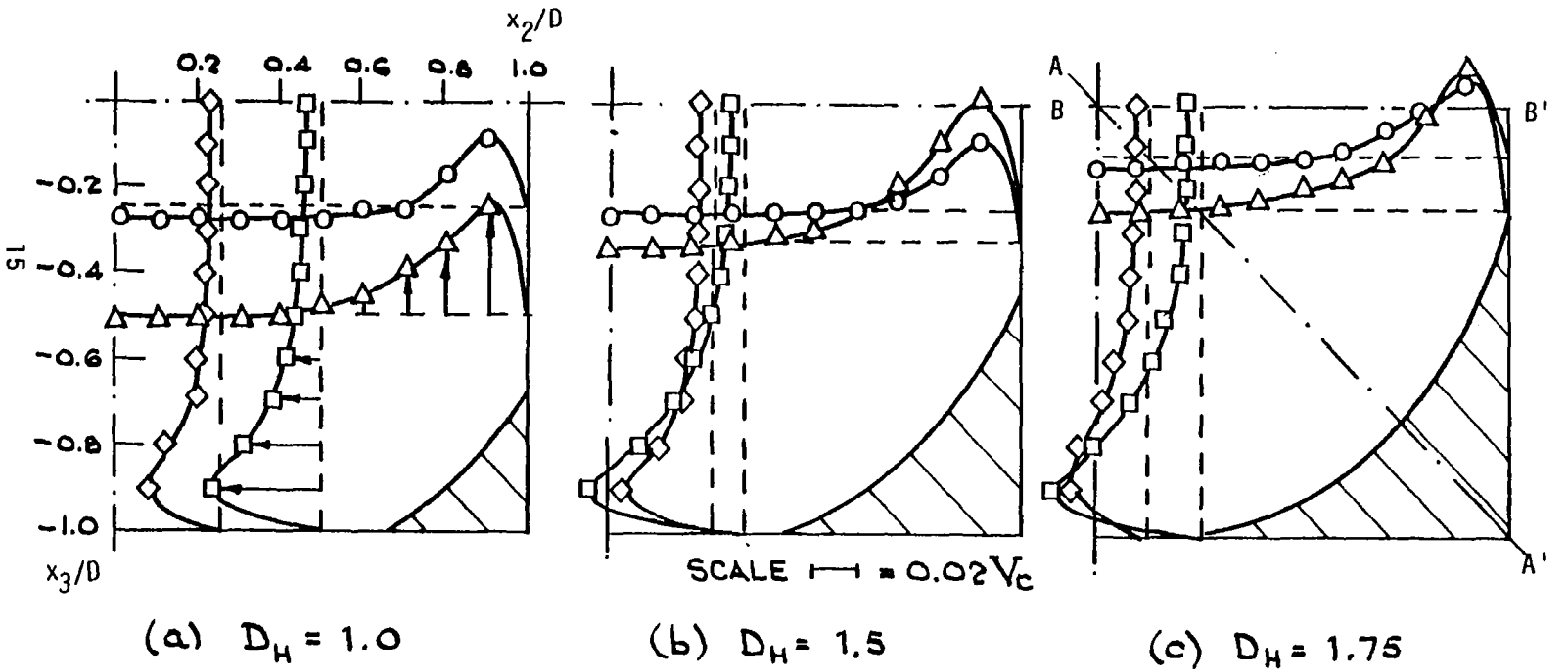

Fig.3 Secondary velocity profiles

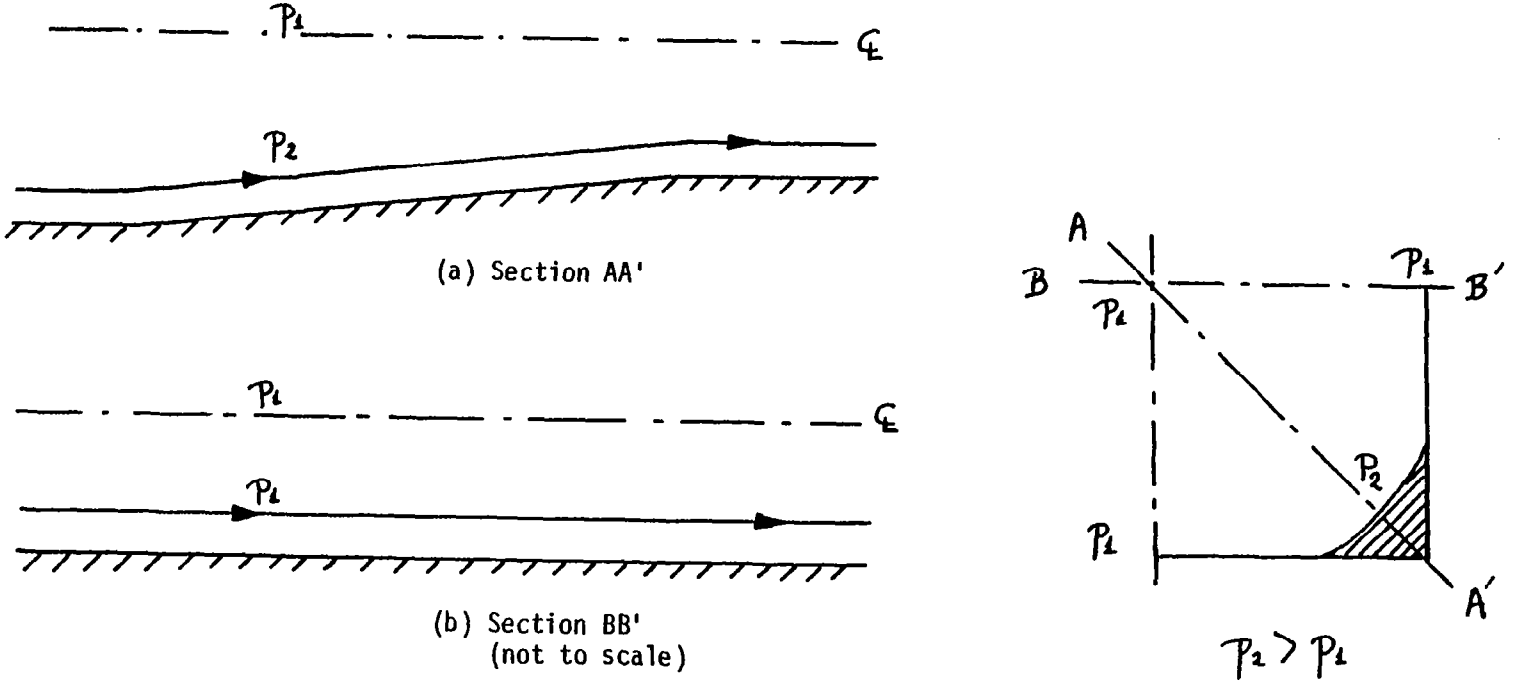

Fig.4 Effect of longitudinal streamline curvature on cross-stream pressure variation

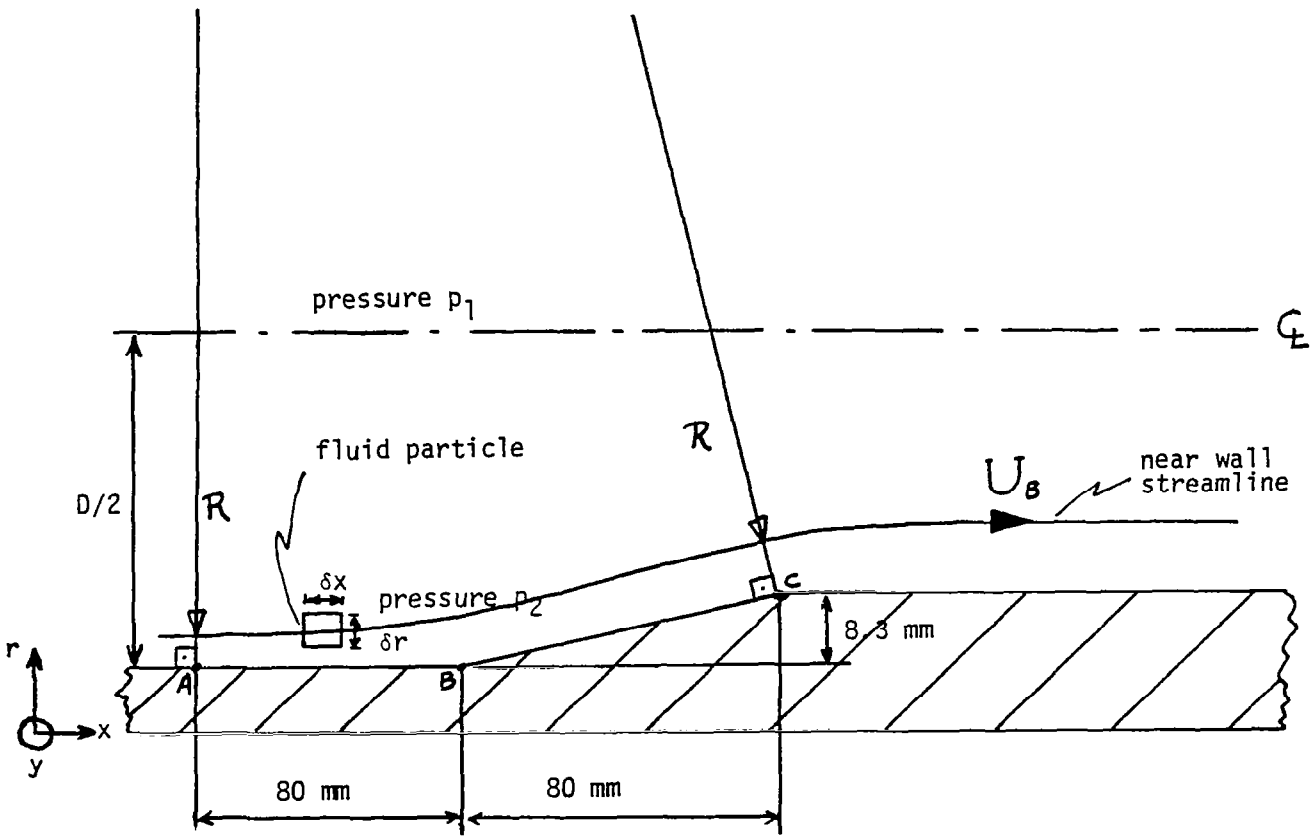

Note: radius of curvature of streamline approximated as radius of circle which inscribes points A, B, C. Hence $R \approx 1.5$ m.

Fig.5 Definition sketch for the estimation of the cross-stream pressure variation (Appendix 2).

1. Report No. NASA CR-3447	2. Government Accession No.	3. Recipient's Catalog No.
4. Title and Subtitle TURBULENT FLOW IN A SQUARE-TO-ROUND TRANSITION		5. Report Date July 1981 6. Performing Organization Code
7. Author(s) A. M. K. P. Taylor, J. H. Whitelaw, and M. Yianneskis		8. Performing Organization Report No. FS/80/30 10. Work Unit No.
9. Performing Organization Name and Address Imperial College of Science and Technology Mechanical Engineering Department Exhibition Road London SW7 2BX, England		11. Contract or Grant No. NASW-3258
12. Sponsoring Agency Name and Address National Aeronautics and Space Administration Washington, D.C. 20546		13. Type of Report and Period Covered Contractor Report 14. Sponsoring Agency Code 505-32-12

15. Supplementary Notes

Final report. Project Manager, Louis A. Povinelli, Propulsion Systems Division, NASA Lewis Research Center, Cleveland, Ohio 44135.

16. Abstract

Measurements of turbulent flow in a duct with a cross-sectional transition from square to round are presented. Laser Doppler velocimetry was used to measure the mean velocity components, turbulence levels and shear stresses. The boundary layers at the inlet and exit of the transition were approximately 13% and 20% of the hydraulic diameter respectively, becoming thicker near the corner fillets. The results show the development of secondary flow, or magnitudes up to 7% of the bulk velocity. This flow is directed away from the corner fillets and along the periphery of the duct and is associated with the longitudinal curvature of the wall and the related pressure gradients.

17. Key Words (Suggested by Author(s))	18. Distribution Statement
Secondary flow Laser Doppler velocimetry Ducts - intake systems	Unclassified - unlimited STAR Category 34

19. Security Classif. (of this report)	20. Security Classif. (of this page)	21. No. of Pages	22. Price*
Unclassified	Unclassified	19	A02

* For sale by the National Technical Information Service, Springfield, Virginia 22161

NASA-Langley, 1981